FTK ROTOR BLADES: DESIGN, MANUFACTURING AND TESTING

Henning Mainz, Rainer Bartels, Bram v.d. Kamp, Oliver Schneider
DLR - German Aerospace Center
Institute of Flight Systems, Institute of Composite Structures and Adaptive Systems
Lilienthalplatz 7, 38108 Braunschweig, Germany

Gerald Kuntze-Fechner, Marc Hahn
Airbus Helicopters Germany GmbH
Industriestraße 4, 86609 Donauwörth, Germany

Abstract

This paper deals with the challenges and particularities of the design, manufacturing and testing of small batch series model rotor blades. It highlights the interaction of dynamic and structural aspects and also compares the different manufacturing technologies that were considered. Subsequently, the final solution, a comparatively simple method to obtain a high quality rotor, is shown. A rating of the new blades and a comparison to Bo105 model rotor blades as well as experiences coming from the wind tunnel tests are presented.

1 Introduction

FTK-META-WK (Advanced Swashplate Concepts-Multiple Swashplate-Windtunnel Test) is a sub-project within the joint research project *Advanced Swashplate Concepts* (FTK) lead by Airbus Helicopters Germany (AHD). The aim of FTK-META-WK was to test the full IBC-functionality of DLR's (German Aerospace Centrer multiple swashplate control system (META) on a model rotor test rig in the large low-speed facility (LLF) of the German-Dutch Wind Tunnels (DNW). In the wind tunnel experiment, higher harmonic control (2-5/rev) tests for noise, vibration and load reduction as well as rotor power enhancement of a four bladed rotor were conducted. Additionally, controllers for inflight-blade-tracking of an unbalanced rotor or dissimilar blades as well as tip-path-plane splitting for BVI-noise reduction were tested [1], [2]. For these purposes, under support of AHD, a new set of modern Mach scaled model rotor blades were designed and built and tested by DLR during the wind tunnel campaign in 2015. One year later within the SKAT project (Scalability and risk-minimization of technology with innovative design) a further test campaign was realized using the FTK model rotor blades and the META on a five bladed rotor.

2 Blade design

2.1 Blade geometry

The FTK model rotor blade was designed as a hingeless, all composite blade with CFRP (Carbon Fibre Reinforced Plastic) skins and a GFRP (Glass Fibre Reinforced Plastic) spar. It was designed to be a 1:2.75 Mach scaled version of the EC145 rotor blade regarding the aerodynamic shape and dynamic behaviour, whereas the root (blade neck) and clamp area (loop) are derived from a Bo105 model rotor blade. The blade root operates as a solid flap and lead-lag hinge whereas the friction of the spar loop between the blade and the blade clamping device acts as a lead-lag damper. Figure 1 shows the outer blade geometry.

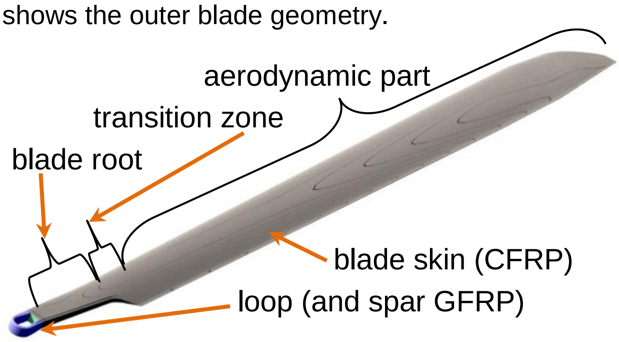

Figure 1: *Outer blade geometry*

2.2 Scaling requirements

The aim of scaling rotor blades to model scale is to match the dynamic characteristics of the full-scale blades. The FTK-blades were aero-elastically scaled in a way that the natural frequencies, in terms of their non-dimensional values in n/rev, are matching the full-scale behaviour for the first three flapping modes, the first two lead-lag modes and the first torsion mode of the EC145 blades. This was done by building a data set for an equivalent beam model of the blade for calculation by a finite element program (FEM). The starting point for the dynamic design was a rough assessment of the structural properties at a small number of 2D-sections of the blade along its radius (see Figure 2).

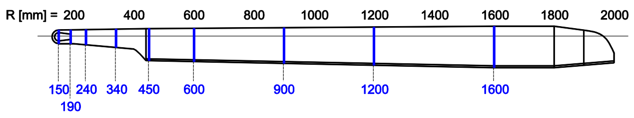

Figure 2: Selected 2D-sections for dynamic design

Thereon, an iterative process between analysis and modification of the data set, with consistent refinement of the 2D-sections and improvement of the results in terms of the objected target frequencies, was carried out. Table 1 shows the final result of the frequency analysis for the FTK-blades as percentage deviation of the values from the original series blades. Deviations in the flapping and torsional frequencies of all modes don't exceed 2%. In contrast, the first lead-lag frequency is clearly increased. This is mainly as a result of the requirements for static and dynamic structural strength and the choice of materials. However, since the first lead-lag frequency has only negligible influence on 4/rev vibration levels and is still within the boundaries set by design guidelines for ground resonance, this value was deemed acceptable.

Rotor radius R	2m
Equivalent blade chord c	0.124m
Airfoil	OA Series
Rotor system	hingeless
Deviation in flapping mode frequency	
1^{st}	+2.0%
2^{nd}	+0.8%
3^{rd}	-1.5%
4^{th}	±0%
Deviation in lead-lag mode frequency	
1^{st}	+16,4%
2^{nd}	+2,8%
Deviation in torsion mode frequency	
1^{st}	±0%

Table 1: Data of Mach scaled FTK-blades

2.3 Dynamic load calculations

For the design of the blades the maximum loads in the wind tunnel tests and the fatigue limits have to be known. For the evaluation of the maximum blade loads a worst case load scenario was defined and the respective loads were calculated using DLR's comprehensive rotor code S4. After an intense search for high load cases from all previous wind tunnel tests performed at DNW-LLF, it turned out that high speed level flights with high thrust at the power limit of the hydraulic unit driving the rotor of the test rig define the worst load cases. Here, the highest loads in flap, lead-lag and torsion occur, increasing from blade tip to the blade root. These loads together with the centrifugal loads extremely stress the blades at the root during operation; therefore this part of the blades had to be investigated carefully for the proof of an endurance limit.

2.4 Blade hull

The design of the outer geometry of the blade is done section wise. Starting points, 2D-sections in chord wise direction with known outer geometry (airfoils, loop, blade root, blade tip, etc.), are selected. In the design software, these sections are then connected with tangentially constant surfaces. To ensure the quality of the resulting surfaces the shapes had to be checked and where necessary improved by supporting geometries to avoid unwanted bulges and dents. The number and positions of these sections depend on the radial profile change. To minimise expense a smaller number of sections are preferable, however a good geometry quality has to be ensured.

2.5 Blade inner structure

Since the outer geometry (Figure 1) is given by the Mach scaling, the design of the inner structure depends on the blade hull. Therefor the blade has to be constructed from the outside to the inside. Most inner geometries interact with and depend on each other. Thus the design of the inner geometry is rather complex and a parametric design is essential to allow for fast changes and multiple iteration loops. A stable parametric design is difficult for many different reasons. Often the design space is not clear in advance and the design software comes with limitations. Like the outer geometry, the inner parts are designed section wise. Often changes to the radial position and further details make additional cross sections necessary for the 3D-design. Some key features and boundary conditions for these cross sections are the outer geometry form, the dimensioning loads and the position of centre of gravity.

The centre of gravity has a huge influence on the aero-elastic stability of the rotor blade and the design of the inner geometry. For aero-elastic stability the centre of gravity of the rotor blade should be located at about 25% cord length or slightly in front of it. The main parts of the rotor blade are the skin, a spar to carry most of the loads and a foam core to support the skin. Since the skin has to cover the complete blade the spar has to be located in the front of the blade. To achieve the target centre of gravity additional high density weights are integrated into the spar.

The adjustment to these and further boundary conditions can only be done in an iterative approach. Some boundary conditions can be addressed directly in the designing process while others have to be determined by further analysis. Iteration can always have an impact on former design decisions and loops. The 2D-sections are used to create a 3D geometry which is mainly used for manufacturing purposes but also allows to derive further 2D sections for their analysis.

Many properties cannot be determined directly in the design process. FE-models have to be built to calculate structural properties and further computations have to be made for the dynamic behaviour of the rotor blade. For this purpose the DLR has developed a set of tools from years of research on rotor blades, especially active twist rotor blades.

SaMaRA - Structural Modelling and Rotor Analysis is a code developed to build parametric FE-Models for rotor blades and calculate their structural properties. It consists of two parts following the two named tasks so that it can be combined with different procedures. Either the FE-Model is generated by the tools' own code or an external FE-Model can be fed to the computational part. The calculations are based on 2D cross sections, which are then extruded for their analysis. Calculated characteristics are for example tension and shear centre, moments of mass and inertia.

This data is used in the FEM-code to calculate the Eigen frequencies for flapping, lead-lag and torsion modes dependent on the rotational frequency of the rotor. This enables the possibility for comparisons with the original rotor blade and critical rotational frequencies can be identified. This step is very important in creating a rotor blade which performs as required and has a stable aero-elastic behaviour (see Table 1).

The last step is to verify the strength of the rotor blade. For this the maximum loads the rotor blade has to withstand were specified as worst case, and described in section 0.

All of these analysis steps are connected with the designing process iteratively. That means each step can bring up results which do not satisfy boundary conditions. This can possibly mean that the design has to be altered at a very early point in the design process. All following steps then have to be repeated. Therefore maximum boundary conditions and knowledge around the rotor blade as possible should be considered as early as feasible to reduce the number of iterations and time.

Finally the inner structure which is shown in Figure 3 was developed.

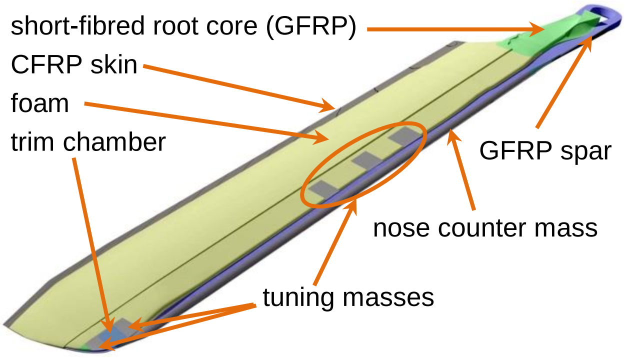

Figure 3: Blade inner structure

Further details and information about the rotor blades design and analysis can be found in [3].

3 Manufacturing

3.1 Method choice

Before the inner design of the blade can start it is essential to select the material to be used and the manufacturing method. Essentially composite components consist of a combination of fibres and resin. Fibre materials can be for example carbon, glass, aramid but also natural fibres as flax or linen.

A composite or fibre reinforced plastic develops when fibres are embedded in resin. In our case it was defined to use glass (spar) and carbon (skin) fibres in combination with a two component epoxy resin.

Fibre materials rovings (fibres bundle -> Figure 4), fabric (woven rovings, Figure 5), non-crimp fabric (rovings side by side fixed for example with filament, Figure 6), and non-woven fibres (e.g. with thermoplastic binder) were used.

Figure 4: Carbon fibres roving

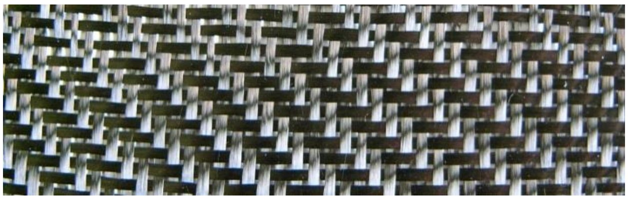

Figure 5: Carbon fibres fabric

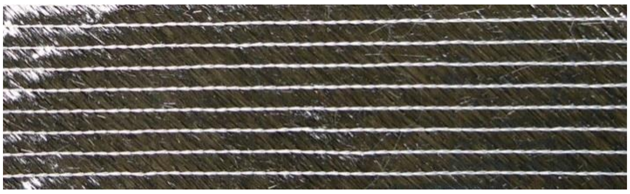

Figure 6: Carbon fibre non-crimp fabric

Figure 7: Carbon fibre non-woven

Two options are in principle available to manufacture a composite part:

1. Resinate the dry fibres. Curing of the material.
2. Use Prepregs. Prepregs are fibres already impregnated with resin (pre-impregnated). Curing of the material.

The resination of the fibres (option 1) can be conducted generally in three different ways:

1. Resinate the fibres by hand using a paintbrush or a foam roll.
2. Injection or infusion of the resin
3. Pultrusion of fibres

Some characteristic unify all composite manufacturing technics: A mould is necessary were the fibres can be applied to and a device to compress the composite material, like a counter block or a vacuum bag is mandatory.

Composite raw fibres can only carry tensile loads in the direction of the fibre orientation like a rope. If they are embedded in resin compressive forces can also be applied. Thus, they have a strong anisotropic behaviour. Consequently, it is possible to design composites exactly according to a load case.

Crucial for the mechanical properties of composites is the amount of fibres in the component, not the resin. The function of the resin is “only” to bond and support. In order to build light weight composite parts high fibre volume contents are required (e.g. 45-60%).

Another important quality factor in terms of loading capacity is the filament straightness. As an example, using non-crimp fabric (nearly perfect straight fibres, Figure 6) higher mechanical strength can be reached in comparison to fabric materials (Figure 5). Accurate laying of the fabric in order to avoid undulation leads to a better result, too.

The weaving of the fabric is crucial for the drapability of the material and has to be chosen suitable to the component geometry in advance.

The following paragraphs describe the four available and partially considered manufacturing methods.

3.1.1 Resination by hand

Using the resination method with a brush or roll is well-established and comparably simple. Nevertheless, if the resination is done carefully it is possible to manufacture high quality composite parts. Resin and hardener are mixed in a given ratio. Usually the processing and the curing are carried out at room temperature. To achieve the final stability often a post curing process (e.g. 55°C for a duration of 16 hours) is required. Despite the temperature treatment the resination by hand is identified as a cold manufacturing process. Figure 8 shows a positive mould (blue) where carbon non-crimp fabric is applied.

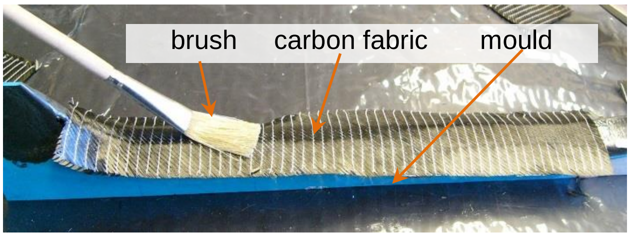

Figure 8: Resination with a brush

In this case the further steps until the final part is ready are:

- Covering the impregnated fabric using a separating foil
- Pressing the layer on the mould by means of a rubber foam block
- Curing
- Demoulding
- Sanding

Finally the desired component is ready for further processing (Figure 9).

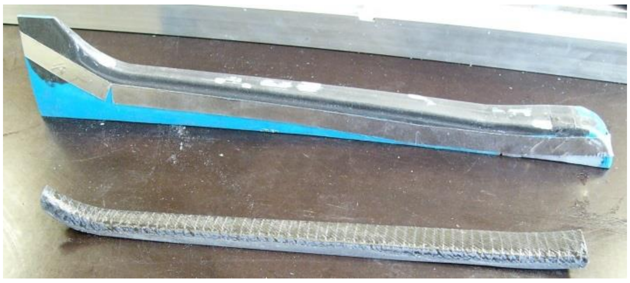

Figure 9: CFRP part and positive mould

Figure 10: CFRP part, interior view

A comparison between Figure 9 and Figure 10 shows the surface quality differences between inner and outer side of the part. The inner part was in contact to the mould. Hence, the surface is a negative copy of the surface of the mould. The outer side was only shaped by a foil and elastic foam, and hence has a much more uneven surface. If both, inner and outer surface have to be smooth, in addition to the rigid mould the use of a rigid form punch is required.

The fibre volume content of handmade composites typically reaches values of up to 35-40% [4]. This can be increased to 60% if the determined amount of epoxy is put into the fabric. Using a brush or a roll for resination causes small air bubbles inside the resin and consequently in the component. Therefore, surfaces of handmade composites suffer from air bubbles and often look shabby, but painting can cover this. However, the impact on mechanical properties is only marginal.

Conclusions:

- Fibre volume content usually between 35-40%; with raised effort up to 60% possible
- Low tooling requirements
- Surface treatment required (air bubbles)
- Lightweight and highly stressable part manufacturing feasible
- Suited for prototype or small batch series
- Equal parts of consistent high quality requires training and qualified workers

3.1.2 Prepregs

Prepreg composites are manufactured by means of an autoclave or by using press moulds. Helicopter manufacturers customarily use press moulds to build their rotor blades in one shot. Depending on the prepreg in use, mostly the curing temperature amounts between 80-180°C. Prepreg processing is a hot-curing method with high demands of the moulds and other utilities like tapes, sealing bands or sealing foils.

The higher the processing temperature is the bigger the impact of different thermal expansion coefficients of the filament, the resin, and the mould on the quality of the composite part. Due to their straightness and fibre volume content between 60-65% [4], prepregs have excellent mechanical properties. Compared to the cold process resination by hand the curing process of prepregs is much faster and the quality of the product is higher. Prepregs are well suited for series production.

In the following a short overview is given for the handling of prepregs using the manufacturing of a model rotor blade skin as an example.

- The required layers of the skin are clipped out of the defrosted material by means of a cutting machine.
- The mould is treated with release agent.
- According to the layout, the layers and finally the tear off sheet are put into the mould (Figure 11).
- During laying, prepregs have an advantageous stick property.

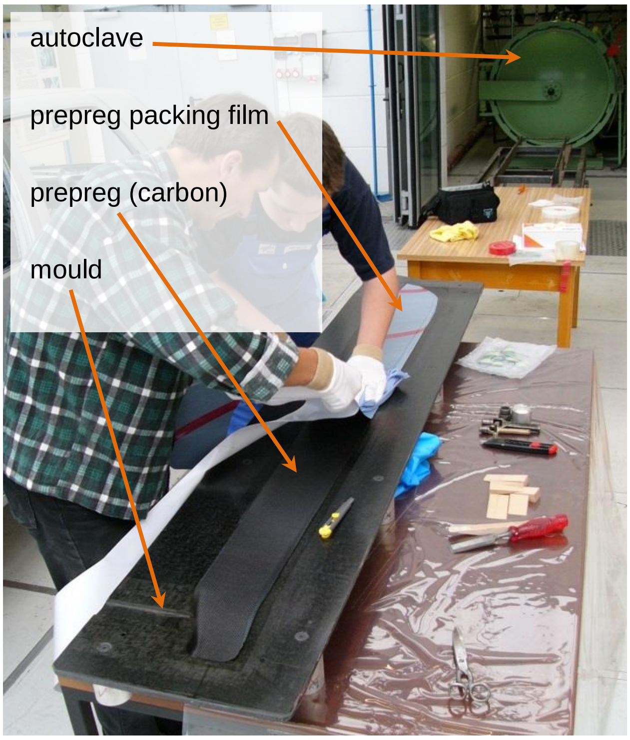

Figure 11: Prepreg laying

- Installation of a vacuum bag (Figure 12 left)
- Curing in the autoclave at 120°C and a pressure of 6 bar.
- Widely unpacked and neatened skin (Figure 12 right)

Figure 12: Vacuum bag (left), cured skin (right)

Conclusions:

- Hot-curing process (e.g. 120°C)
- High fibre volume content (60-65%)
- High quality component manufacturing
- Autoclave required
- High demands on the mould (temperature, pressure)
- Well established for batch manufacturing

3.1.3 Resin transfer moulding (RTM)

At the resin transfer moulding the dry fibre material is put into the mould. A suction and a resin line are installed and finally everything is covered with a vacuum foil. Now while the resin line keeps closed the fibre material is evacuated by means of a vacuum pump. After this the resin line is opened and the resin flows into the cavities. In our case the vacuum line consists of a spiral which is covered by a semi-permeable hose that allows passing air but blocks liquids (MTI® hose, **M**embrane **T**ube **I**nfusion, Figure 13). Therefor the vacuum pump is protected from resin.

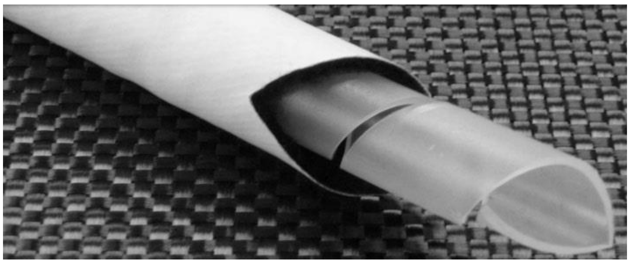

Figure 13: MTI® hose [5]

Figure 14 shows an infusion of a carbon fibre model rotor blade skin in process.

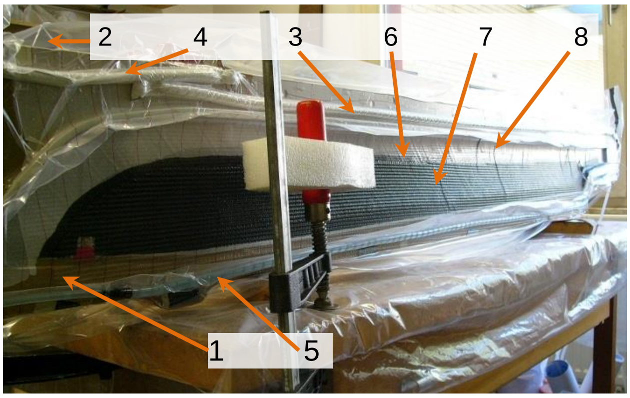

Figure 14: Infusion of a CFRP component

Process of the infusion:

- The picture shows the aluminium mould (1) and the infusion build up. The resin processing is executed at room temperature.
- Evacuation of the vacuum bag (2) by means of a suited pump. The vacuum line (3) is a MTI® hose in order to protect the pump from resin. A manometer which is connected to a second MTI® hose (4) serves as vacuum monitor.
- When the evacuation level is sufficient the resin line can be opened. The resin comes from a reservoir and flows through a plastic pipe connected to a plastic spiral (5).
- The border (6) between resinated (7) and dry (8) material is well-defined.

Conclusions:

- Fibre volume content between 40-50% [4]
- Suitable for cold and hot-curing processing
- Simple handling
- Bubble free parts ➔ good mechanical properties and perfect surface
- Suited for prototype and batch series (latter requires higher tooling)

3.1.4 Pultrusion

By the pultrusion method, roving bundles are pulled through a resin filled impregnation bath and afterwards through calibration rolls or nozzles. From a technical point of view the outcome of this are prepregs. By the pultrusion device (Figure 15) a fibre volume content of 50% can be reached.

Features of the process of the pultrusion:

- The required quantity of roving spools (not visible in Figure 15) is mounted to a rack (1).
- The roving guidance (2) is a metal block with holes to arrange the rovings side by side.
- The rovings are guided along a big drum (hidden) thru the resin reservoir (3)
- By means of a variable spring tension (4) the fibre volume content can be adjusted using the corresponding calibration rollers (5)
- With the aid of the shape calibration rollers (6) width and thickness of the rectangular tape (impregnated roving) can be adjusted.
- Merged roving bundle (7)
- A winch with a rope and a plier are used to pull the roving bundle through the machine.

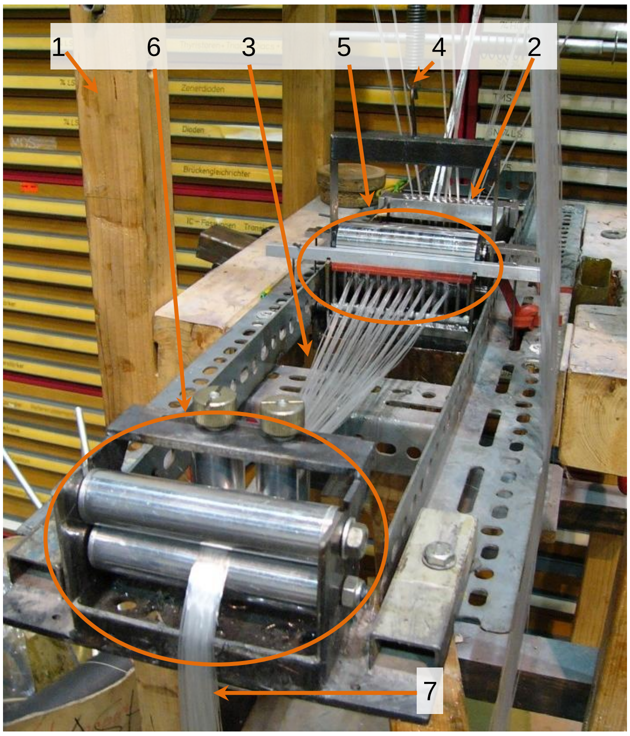

Figure 15: Pultrusion device with roving bundle

Conclusion:

- Fibre volume content around 50%
- Preferential for cold-curing epoxy
- Comparable simple handling
- Suitable for unidirectional tape manufacturing
- Suited for prototype or small batch series

3.2 Thermal effects

The thermal behaviour has a big influence on the blade manufacturing method choice. Aluminium, the basic material for the mould, has a thermal expansion coefficient of $23.8 \cdot 10^{-6}$/K [6] in each direction. In contrast, the thermal expansion coefficient of high tension carbon in fibre direction amounts to $-0.5 \cdot 10^{-6}$/K and $30 \cdot 10^{-6}$/K perpendicularly [4]. The thermal expansion of multidirectional carbon composites is dominated by the thermal expansion behaviour along the fibres and amounts to approximately $0 \cdot 10^{-6}$/K.

What happens to a composite part made of carbon prepreg when it is manufactured in an aluminium mould at 120°C is quite simple. The calculation of the elongation of the aluminium mould with a supposed length of two meters at a temperature difference (relative to room temperature) of 100K results to:

$$\Delta L = 2000mm \cdot 23.8 \cdot 10^{-6} \cdot 100K = 4{,}76mm$$

During curing, the carbon part adapts to the shape of the mould deformed by temperature. After the curing of the carbon, everything is cooled down to room temperature. Due to the different thermal expansion coefficients the aluminium mould shrinks to its original size but the carbon part does not. Hence, the carbon does not fit into the mould any longer. If it is required that the hot processed carbon part fits into the mould at any temperature, it's an option to use a mould made from carbon or Invar® steel. Both, carbon and Invar® steel behave similarly. Unfortunately, the mould manufacturing costs would increase considerably.

3.3 Method rating

For the rating the most relevant blade manufacturing boundary conditions are summarized as follows:

- The skin of the rotor blades will consists of carbon fibre reinforced plastic.
- The spar will consist of unidirectional glass fibre reinforced plastic.
- The mould material will be aluminium.
- Only a small batch will be manufactured.
- Main requirement: the output of high quality blades with minimized manufacturing risk.

The rating considers blade manufacturing using prepregs (hot-curing process) as well as a cold-curing process. Four options are available:

1. Blade manufacturing in one shot using prepregs.
2. Blade manufacturing in steps using prepregs.
3. Resination of the skins by hand. Pultrusion of the spar. Manufacturing in steps.
4. RTM resination of the skins. Pultrusion of the spar. Manufacturing in steps.

Four general criteria are applied to the manufacturing option:

a) Experiences at DLR
b) Component quality
c) Manufacturing complexity
d) Thermal expansion coefficient impact

3.3.1 Option 1:

The manufacturing of the blades in one shot with prepregs is state of the art, suited for volume production and promises high quality blades. Thermal expansion effects have to be considered. According to AHD a lot of prototypes are necessary before the method runs smoothly. DLR has no experiences with this very complex method.

3.3.2 Option 2:

A multistage blade manufacturing with prepregs is in principle possible, suited for small batch series which has been used at DLR. Since adjustments during the manufacturing are possible the complexity is not that high. Thermal effects have a big impact, whereby the blade quality suffers.

3.3.3 Option 3:

In applying the (at DLR) well-known cold-curing process, different thermal expansion coefficients have no effect on the blade quality. The optical quality of the blade skins suffers from air bubbles (resination by hand) and requires additional finishing works. Using this multistage suitable manufacturing method, only a few pre-tests and prototypes are required until this comparably time-consuming – and thus only suited for small batch series – blade manufacturing can start.

3.3.4 Option 4:

Except for the skin manufacturing, option 4 conforms to option 3. The RTM method (state of the art and suited for skin manufacturing), is in principle known at DLR, promises high quality surfaces but has to be trained until the process works well.

3.3.5 Result

Considering all options and boundary conditions, option 4 was selected for the blade manufacturing. Even though this method is comparably time-consuming and is not suited for batch processing, it promises the lowest risk and costs in combination with the best result.

3.4 Blade manufacturing steps

The blade consists of several parts which are manufactured and cured separately. Only the spar and the short-fibered root core are non-cured parts which are build-in during the final assembly.

3.4.1 Skins

The skins of rotor blades are mainly designed to carry torsion loads. Thus, predominant carbon layers with ±45° fibre orientation are used. The skin resination is done by RTM. Several preparative steps are necessary in advance of the impregnation with resin. First, the mould has to be cleaned and treated with release agent. Areas where contact with resin should be avoided have to be covered with tape or filled up with modelling clay (Figure 16, left). Then the fibre material is applied and fixed with spray adhesive. The right side of Figure 16 shows the dry carbon fabric inside the mould.

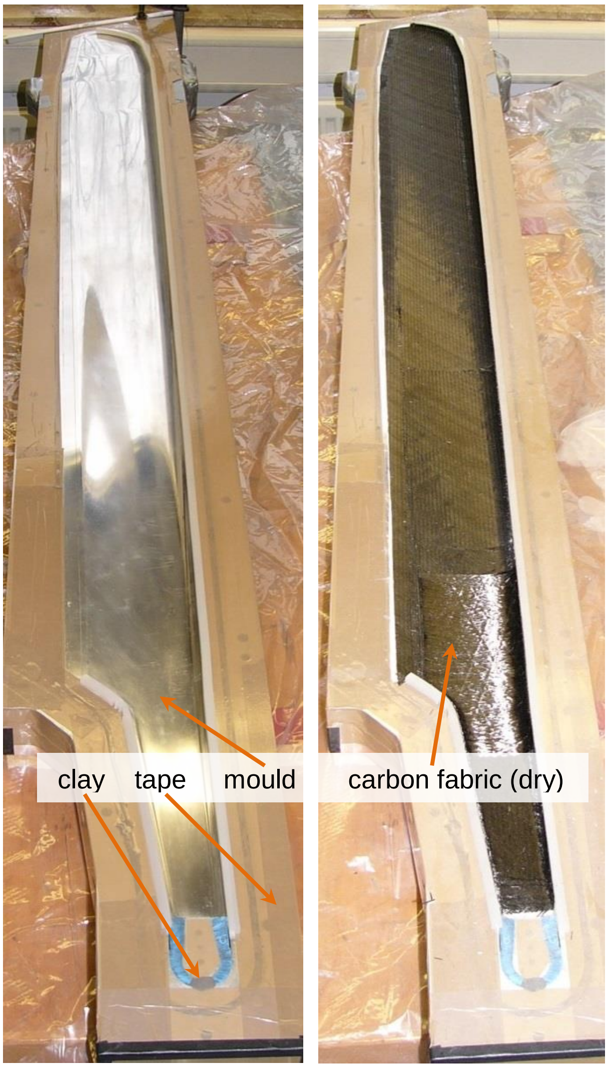

Figure 16: Skin manufacturing, first steps

After that, the infiltration setup starts with a tear off sheet layer. After curing and removal, tear off sheets (marked with red stripes, see Figure 17), ensure a surface with very good bonding properties. A foil with a lot of small holes is following. This foil forms a separating layer in order to ease the unpacking of the auxiliary material. A flow promotor, which comes next, eases and accelerates the resin entry into the dry material (half impregnated, visible in Figure 17).

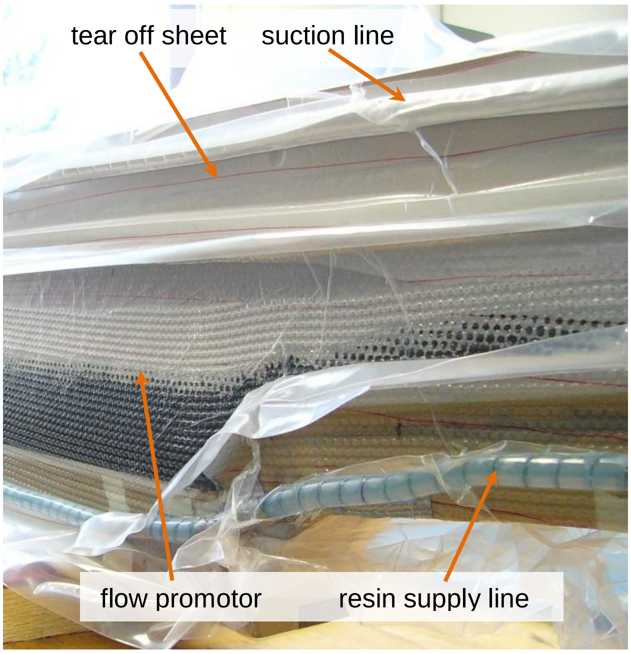

Figure 17: RTM setup

Then, the resin supply and the suction lines are installed. Finally, the whole is covered by a vacuum bag. Starting the process, the vacuum bag is evacuated and the resin supply will be enabled. The process ends, when everything inside the vacuum bag is impregnated.

After curing of the part at room temperature everything is removed, except for the skin. Overhang composite is neatened by means of suited tools like an oscillating saw and a chisel.

Figure 18 shows the root area next to the loop of a final neatened skin.

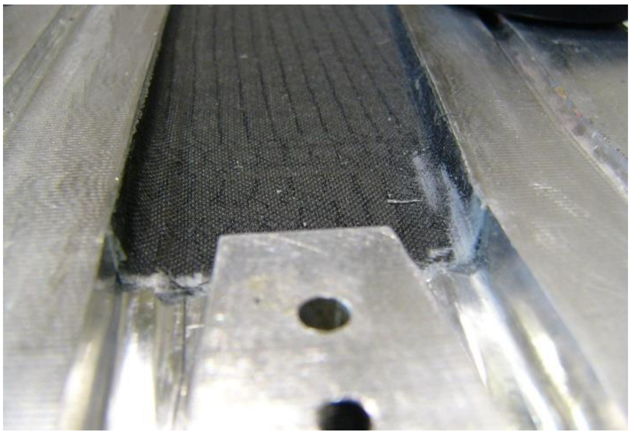

Figure 18: Neatened blade root area

This step is quite time consuming and has to be completed with high attention in order to keep the skin in the mould. Compared to the preparation and finishing works the resination itself is not very time-consuming.

3.4.2 GFRP spar

The main function of the spar is to carry the centrifugal loads. In such a one-dimensional load case, unidirectional fibres are the best choice.

The raw spar material was produced using the pultrusion device presented in paragraph 3.1.4 (Figure 15). From the calculation the spar was intended to have a fibre volume content of 50%. In reality the value of the produced strings fluctuates between approximately 47 and 52%. This unimportant inaccuracy allows for the manufacturing of high grade spars. The orange part visible in Figure 19 represents the virtual view of the upper half of the spar.

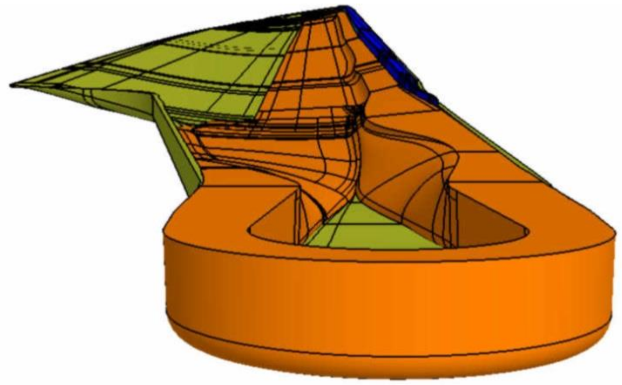

Figure 19: Shape of the upper half of the spar

The loop has an almost rectangular cross section which crosses over to one half of a c-shaped spar in the aerodynamic blade section. The spar half consists of six rectangular glass fibre tapes which have to be guided and distributed in a certain way. The crucial area is the cross over from the loop to the aerodynamic blade section where the GFRP tapes are turned from vertical to horizontal orientation. This process is shown in Figure 20 for the first of the six glass tapes of one half of the spar.

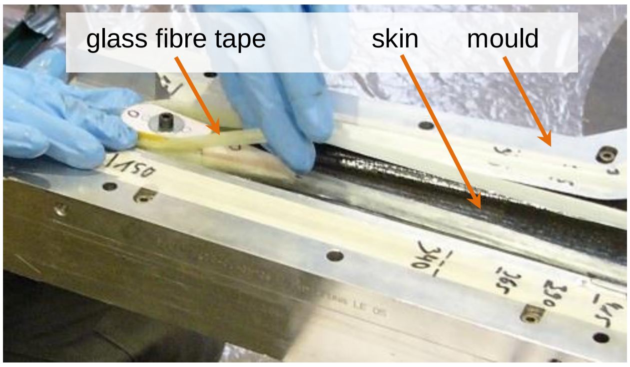

Figure 20: Glass fibre tape during deposition

The tapes are positioned by means of templates in order to reach the shape of the spar shown in Figure 19.

3.4.3 Torsion lid and nose counter mass

The lid connects the upper and lower skin in order to close the torsion cross section. It extends to nearly the whole aerodynamic part – except the parabolic blade tip – and was manufactured by hand with a carbon fibre volume content of 45%.

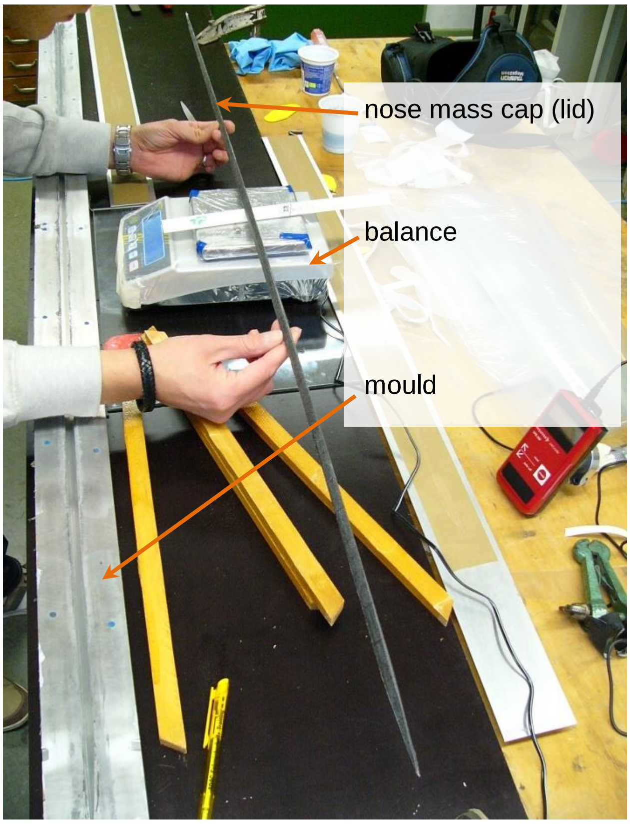

Figure 21: Nose mass cap trimming

The inner space of the lid is filled with a mixture of tungsten and epoxy and provides a chord wise centre of gravity ≤ 25%. All nose mass caps were trimmed to the same weight and to the same radial centre of gravity. Figure 21 shows one cap during the trimming procedure.

3.4.4 Foam

The foam fills the inner cavities of the blade's aerodynamic section between the skins and the spar. It has to be milled on both sides, making the manufacturing comparably costly. The foam provides the needed pressure during the final assembly of the blade. Figure 22 shows the foam lying inside the upper skin of the blade.

Figure 22: Foam

The notches in the foam are reserved for several tuning masses and a trim chamber.

3.4.5 Tuning masses

Five milled span wise distributed tuning masses made of sintered tungsten with a density of 18.5g/cm^3 are designed to match the desired dynamic blade properties.

3.4.6 Trim chamber

The trim chamber (Figure 23, left) near the blade tip can be filled up with plumb or tungsten to balance blade mass dissimilarities. It is positioned between the outer trim masses and consists of some tubular carbon fabric layers. These hand resinated hoses are pressed against the walls of a negative mould by means of a balloon during the curing of the resin.

3.4.7 Blade neck caps

After assembly and curing of the blade (see section 3.5), the blade neck caps (Figure 23, right, manufacturing shown in chapter 3.1.1) are bonded to the blade neck in order to close the torsion cross section.

Figure 23: Trim chamber and blade neck caps

3.4.8 Temperature treatment

In order to reach the final composite properties a temperature treatment was required. This happened inside a temper oven, a big Styrofoam chamber with a temperature controlled fan heater at 55°C for 16 hours.

3.4.9 Finishing

A lot of work is required to give the blade the final shape. All overlapping material has to be removed. The blades nose area needs an especially careful job in order to reach the aerodynamically required accuracy.

3.4.10 Blade shoe

In order to be able to mount the rotor blades to the rotor head a blade shoe is necessary. Supported by a special rack the loop of each blade was glued into the aluminium blade shoe (Figure 24).

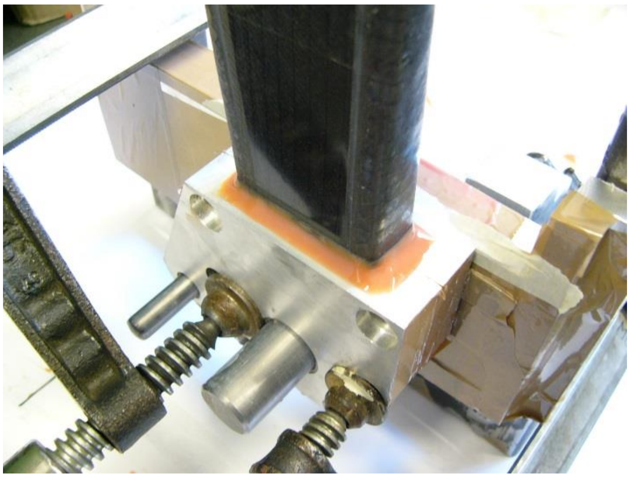

Figure 24: Blade shoe mounting

3.4.11 Instrumentation

The FTK rotor blades are instrumented with strain gauge bridges at the blade root and one torsion bridge inside the blade at 35% span. These gauges have blade monitoring purposes to ensure safe operation in every test condition.

3.5 Blade assembly

The final assembly of a blade starts with the manufacturing of the spar. The starting point is shown in Figure 25. Before this stage is reached, several preparation steps are required.

1. Manufacturing of the skins, the integrated nose mass cap, the trim chamber, the blade neck caps, the foam, and the tuning masses.
2. Glue the nose mass lid into the upper skin.
3. Insert a removable nose mass dummy into the lower skin as boundary for the spar manufacturing.
4. Insert removable spar rear edge guide bars into the skins.
5. Prepare all templates and spar inspection jigs.

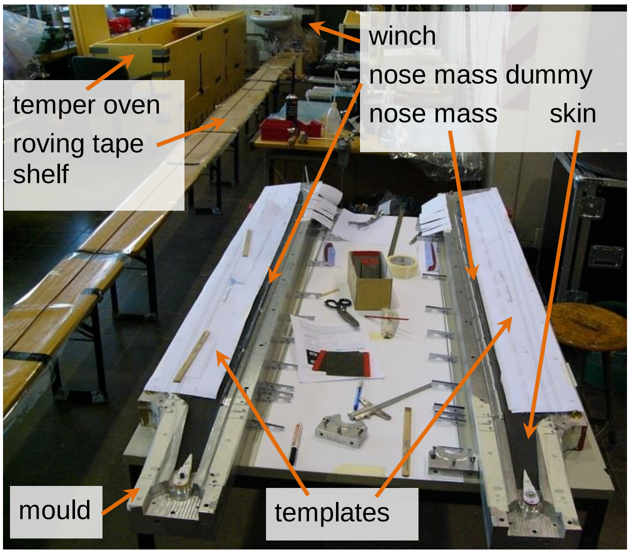

Figure 25: Blade assembly preparation

At this point, the pultrusion device is filled with resin and the manufacturing of the GFRP tapes starts. The impregnated tapes are laid down to the shelf. With the help of foldable templates made of paper, the positions of the tapes are given and the build-up of the spar halves is done step by step.

Finally the inner shape of the spar is checked with a lot of jigs, as visible in Figure 26, and corrected if necessary.

Figure 26: Spar geometry check

Then all supporting tools are removed and the blade neck areas are filled up with a mixture of resin and short fibres (Figure 27).

In the next steps, the foam is glued into the upper blade half, then the tuning masses and the trim chamber are glued in. Finally the contact areas of upper and lower blade half and remaining cavities are brushed or filled with thickened resin. By means of a crane the lower side of the blade lying in its mould half is lifted, carefully turned and then lowered to meet the upper blade half. Figure 27 shows the blade shortly in advance of the blade half conjunction.

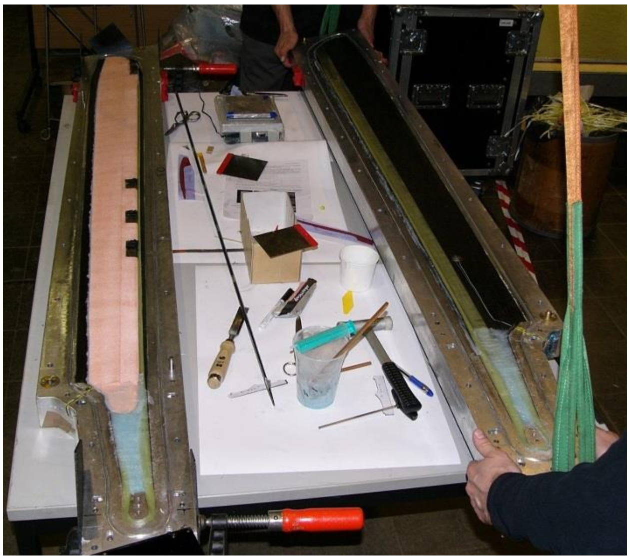

Figure 27: Blade before final assembly

Directly after the conjunction of the blade halves the closed mould is put into the temper oven for curing and temperature treatment, before the blade neck caps and the blade shoe can be applied to the finished blade (see paragraphs 3.4.7, 3.4.8, 3.4.9, and 3.4.10).

4 Results

4.1 Optically

After the temperature treatment, the mounting of blade root caps and the blade shoe, the installation and calibration of the external strain gauge bridges, application of the SPR (stereo pattern recognition) dots, the final finishing, pre-test at a whirl tower and the balancing, the rotor blades are ready for use. The surface finish of the blades (two blades are shown mounted to the wind tunnel model in Figure 28) is very good. For the wind tunnel test, the blades were not repainted, only partly polished.

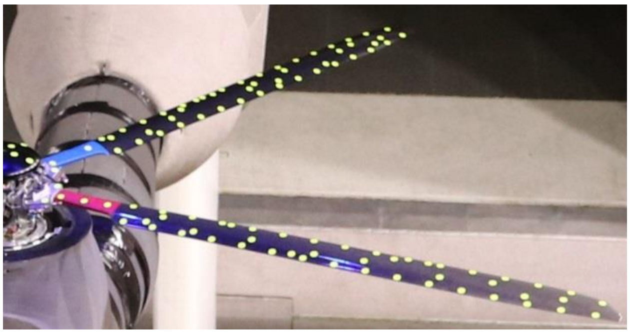

Figure 28: FTK/SKAT rotor blades

Due to the cold manufacturing process, the skins of the blades remained inside the mould until the final assembly. Consequently, the blade halves fit together perfectly. In particular the shapes of the blade noses are very good.

4.2 Blade laboratory tests

For the whole design process a multidisciplinary design chain was established at DLR to satisfy all boundary conditions. Since the goal of the dynamic design was to manufacture new blades and not only to get data for simulation applications, the output of this design chain was a full 3D-model of the blade containing all the necessary information about the composite lay-up and the material properties. Upon completion, the blades were first CT (computer tomograph) scanned at AHD to find out possible weak points in the structure for example cavities or kinks in the rovings and so on. After that, the blades were equipped with strain gauges on the blade root for measuring the blade loadings and then single tested on a whirl tower at DLR up to 115% nominal RPM. The strain gauges were also used to determine the natural frequencies of the finished blades in flap, lead-lag and torsion. In Figure 29 the frequencies of the lower Eigen modes of the FTK-blades are plotted against the rotational speed of the rotor.

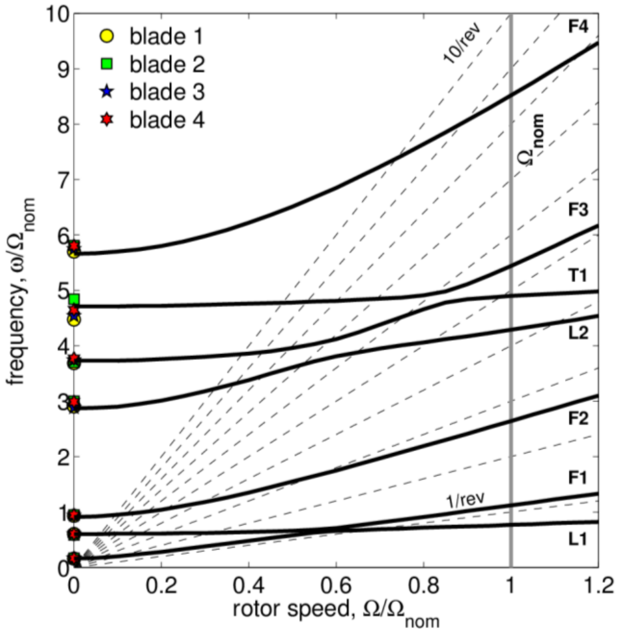

Figure 29: Fan diagram

The measured non-rotating frequencies of all four blades used in the wind tunnel test are also plotted in the same figure. As can be seen, the results of these measurements are almost congruent with the target values at 0 rpm. The blade-to-blade differences of the bending modes are virtually negligible. Only in torsion small variations are visible. All in all the blades build satisfies the target design and should therefore have an identical dynamic behaviour compared to the original series blades.

5 Wind tunnel experiences

On the basis of three wind tunnel test cases it will be shown how the FTK blades behave in comparison to the Bo105 blades.

5.1 Thrust polar

At the beginning of the tests of each rotor a thrust variation without wind was performed. For the Bo105 blades rotor the thrust was changed between 0 N and 6000 N. Due to an increasing unbalance of the rotor the thrust level could not be raised further. Using the FTK rotor, the thrust variation was performed between 0 N and 7000 N as planned in the test matrix.
In Figure 30 the unbalance behavior of both rotors is shown (1/rev Cosine and Sine component of vertical load cell No #1 of the rotor balance) for the thrust range of 0 N up to 6000 N in steps of 500 N. For the nominal thrust of about 4000 N used during the wind tunnel test the unbalance of both rotors is as low as expected. As can be seen, there is a steep raise of the unbalance with increasing thrust for the Bo105 rotor. For the FTK rotor the unbalance remains relatively low over the complete range.

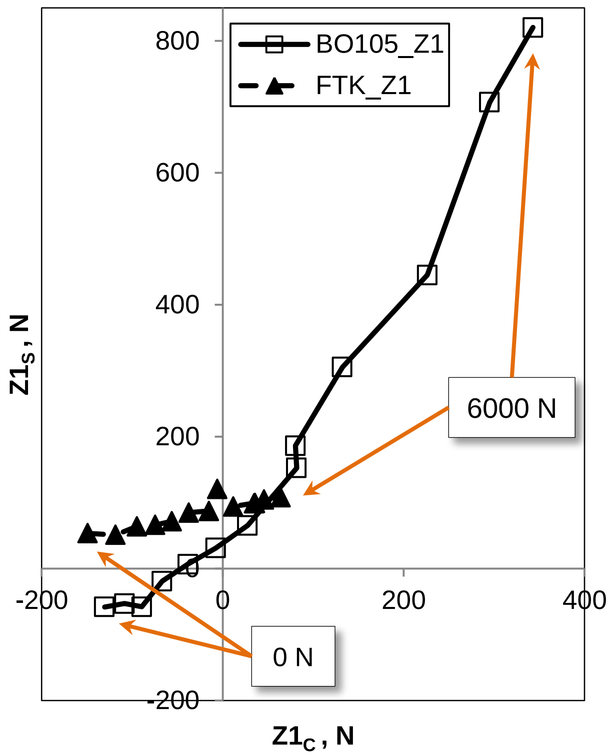

Figure 30: Unbalance behavior of both rotors

This behavior can be explained by comparing the blade deformation results obtained from the optical SPR [7] measurements. It could be noted that the blade to blade differences in blade tip lag deflection are varying by about 5 mm for the FTK rotor but by about 25 mm for the Bo105 rotor. A change in blade to blade lag displacement leads to a shift of the center of gravity of all four blades and finally results in an increased unbalance.

5.2 Figure of merit

A performance comparison for both rotors is shown in Figure 31. As expected, the Figure of merit calculated for the FTK rotor surpassed the value for the Bo105 model rotor especially at higher thrust levels. Accordingly, the power needed to hover at a thrust of T = 6000 N was 6.3% lower for the FTK rotor than for the Bo105 model rotor.

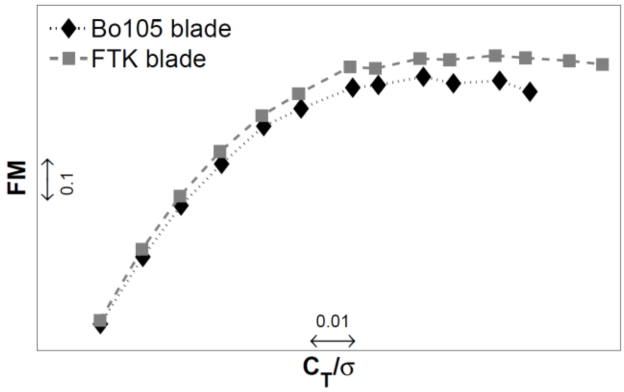

Figure 31: Figure of merit for Bo105 and FTK rotor

5.3 Blade deformation in descent flight at Higher Harmonic Control

In the following, the reaction of the FTK and the Bo105 rotors on Higher Harmonic Control inputs is compared on the basis of SPR results. Figure 32 shows a summary of the measured n/rev mean pitch amplitudes in the descent flight condition (μ = 0.15) for both rotors. Looking at the n/rev amplitude change in comparison to the radial position it can be noticed that the FTK rotor blades show only a small increase over the radius (+3% at 2/rev up to +70% at 4/rev) compared to the Bo105 model blades (+46% at 2/rev up to +200% at 4/rev).
This can be explained by the difference in torsional stiffness of the rotor blades. The first torsion frequency of the Bo105 blades is at 3.5/rev compared to 4.7/rev for the FTK blades. For this reason, the amplitude increase over the radius starts at higher input frequencies for the FTK rotor.

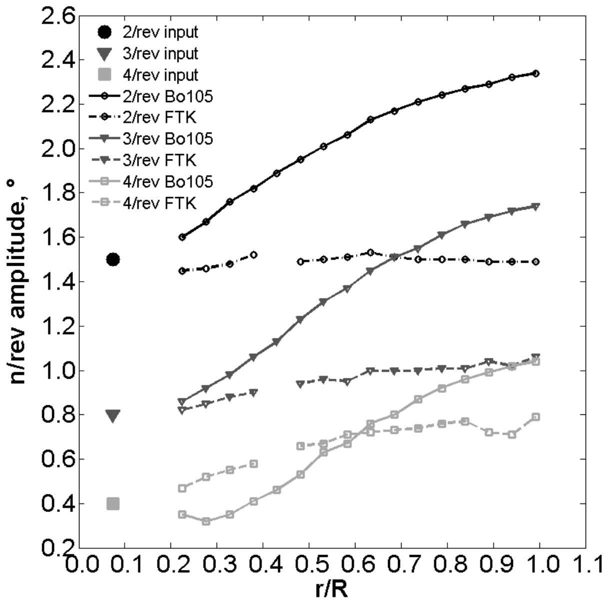

Figure 32: n/rev pitch amplitudes at μ=0.15

This behaviour is also visible in the n/rev phase plot over radius, as shown in Figure 33. With increasing HHC input frequency the phase delay also increases for both rotors. The comparison of the maximum delay shows relatively small values for the FTK rotor (+5° at 2/rev up to +20° at 4/rev) but high values for the Bo105 rotor from +17° at 2/rev up to 105° at 4/rev pitch input.

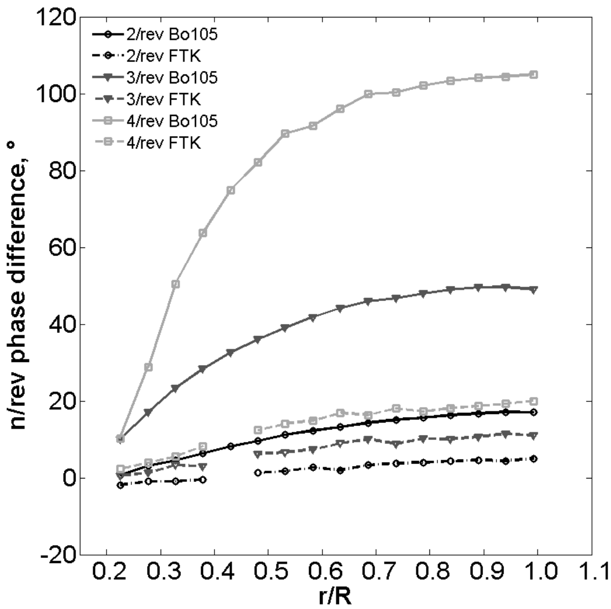

Figure 33: n/rev phase delay at μ =0.15

6 Conclusion and future outlook

DLR Braunschweig has conducted wind tunnel tests for decades with whole helicopter model configurations and new model rotor blades. The dynamic design of rotor blades is well-known. Experiences with the treatment of composite material have also existed for a long time. Nevertheless the following improvements were made.

- For the whole design process of Mach scaled model rotor blades a multidisciplinary design chain was developed and established at DLR to satisfy all boundary conditions for save operations in wind tunnel experiments.
- Essential for the success of the project was the decision to use a cold curing and a stepwise manufacturing process for the rotor blades. Therefore thermal expansion effects between the mould and the composite materials had no influence. Beside this the requirements on the tooling are comparably small.
- If only a small amount of parts are needed the manufacturing time for a single part is not critical. It is more important to optimize the whole manufacturing process in order to reach the goal time and to be cost efficient. For this reason DLR developed a new (for DLR) manufacturing method in steps with pre-cured infused skins and a blade assembly with a pultruded not cured spar.
- Using the presented RTM method which becomes more and more important for industrial application, parts with high mechanical and optical qualities can arise. The assembly with a soft core (spar and thickened resin) has the advantage that in combination with the foam the inner structure can slightly move before curing and everything finds its right position.

Consequently a new set of modern model rotor blades (FTK-blades) was manufactured at DLR with the support of AHD. These rotor blades are aerodynamically, dynamically, geometrically and optically of very high quality and were successfully tested in the wind tunnel and showed excellent performance.
Because of this very good experience future blade sets will be manufactured, if possible, in the same manner. In order to receive more information from the rotor the next blades will be equipped with dynamic pressure sensors whose installation and wiring represents a particular challenge.

Acknowledgements

The authors would like to thank the team at Airbus Helicopters for their support in designing the new model rotor blades used for the test and their endorsement of this publication. The tests in the DNW wind tunnel were conducted within the framework of the national research project FTK (advanced swashplate concepts) funded by the German Federal Ministry of Economic Affairs and Energy (BMWi).

Supported by:

Federal Ministry
for Economic Affairs
and Energy

on the basis of a decision
by the German Bundestag

References

[1] Küfmann, P., Bartels, R., Wall, B. G. v. d., Schneider, O., Holthusen, H., Gomes, J., Postma, J.: “The First Wind-Tunnel Test of the DLR’s Multiple Swashplate System: Test Procedure and Preliminary Results”, 72nd Annual Forum of the American Helicopter Society (AHS), West Palm Beach, Florida, May 2016

[2] Bartels, R., Küfmann, P., Wall, B. G. v. d., Schneider, O., Holthusen, H., Gomes, J., Postma, J.: “Testing Active Rotor Control Applications using DLR’s Multiple Swashplate Control System in the LLF of DNW”, 42nd European Rotorcraft Forum (ERF), Lille, France, Sept. 2016

[3] van de Kamp, Bram; Kalow, Steffen; Riemenschneider, Johannes; Bartels, Rainer; Mainz, Henning: “Multidisciplinary Design Chain for model rotor blades”, ICAS 2016 - International Council of Aeronautical Sciences - Proceedings. Daejon, Südkorea.

[4] Heinrich W. Bergmann, “Konstruktionsgrund-lagen für Faserverbundbauteile”, Springer Verlag, ISBN 3-840-54628-6

[5] DD Compound, Lengericher Straße 8, 49479 Ibbenbüren, Germany, www.dd-compound.com

[6] Tabellenbuch Metall, 37th Edition, Europa Lehrmittel, ISBN 3-8085-1107-9

[7] O. Schneider, “Analysis of SPR measurements from HART II”, Aerospace Science and Technology, vol. 9, no. 5, pp. 409–420(12), 2005